

**Figure 12.** Inverse correlation of  $k_2$  for phenol (O) and toluene (□) in 1-PrOH/water mixed solvents with optical absorption energy  $E_r$  of  $e_s^-$  in zones b and c.  $T = 298$  K.

of bound excited states (probably 0, 1, or 2) of the electrons in the solvation potential wells is the same in each of the 1-PrOH/water mixed solvents, the ground-state electron trap depth is related to the optical absorption energy.<sup>31</sup> The great breadth

of the optical absorption band indicates that all of the electrons are not in traps of the same depth in a given liquid. Electrons in the shallower traps have a greater probability of reacting per unit time than do those in deeper traps. An indicator of trap depth for kinetics purposes is taken as  $E_r$ , the optical absorption energy half way up the low energy (red) side of the band.

$$E_r = E_{\epsilon_{\max}} - W_r \quad (5)$$

where  $W_r$  is the portion of the band width at half-height that is on the red side of the band maximum.

Values of  $E_r$  in 1-PrOH/water mixed solvents, calculated from data in ref 19 and 24, are given in Figure 11. Zones a, b, and c are visible, but zone d is not. The value of  $E_r$  increases with increasing water concentration through zone b and decreases through zone c. This correlates inversely with the concomitant changes of  $k_2$  (Figure 12), as expected. The rate constants in zones a and d, which border the single component solvents, do not fit the correlation with  $E_r$ . The study continues.

**Acknowledgment.** We are grateful to the Natural Sciences and Engineering Research Council of Canada for financial assistance, and to the staff of the Radiation Research Center for construction of the apparatus.

**Registry No.** 1-PrOH, 71-23-8; H<sub>2</sub>O, 7732-18-5; nitrobenzene, 98-95-3; acetone, 67-64-1; phenol, 108-95-2; toluene, 108-88-3.

(31) Jortner, J.; Noyes, R. M. *J. Phys. Chem.* **1966**, *70*, 770.

## Oxidation of Diphenylamine by OH Radicals and Excitation of the Diphenylamino and OH Adduct Radicals

K. H. Schmidt, A. Bromberg, and Dan Meisel\*

Chemistry Division, Argonne National Laboratory, Argonne, Illinois 60439 (Received: March 28, 1985)

The primary product of the OH reaction with diphenylamine (DPAH) is a mixture of OH adducts (DPAH·-OH) which subsequently eliminate OH<sup>-</sup> ions via a pH-independent and an acid-catalyzed process. The rate constants of these two processes have been determined. The acidic amino radical cation (DPAH<sup>+</sup>·) thus obtained has a  $pK_a$  of 4.2. The adduct, the amino radical cation, and the neutral amino radical (DPA·) were excited with frequency-doubled ruby laser pulses (347 nm). The excited states of the latter two amino radicals are shorter lived than the presently utilized laser pulse. Furthermore, no laser-induced shift in the acid-base equilibrium of DPAH<sup>+</sup>·/DPA· could be observed. This lack of laser excitation effect leads to the conclusion that the difference in acid-base equilibrium constants ( $\Delta pK_a^*$ ) of the ground vs. the excited state is substantially smaller in the radical than in the analogous singlet states of the parent amine molecule. Förster cycle considerations based on the absorption spectra of the two forms of the radical substantiate this conclusion. Excitation of the OH adduct leads to OH<sup>-</sup> elimination from the excited state. This elimination leads to production of the amino radical cation in its ground state. Relaxation of this laser-induced perturbation of the acid-base equilibrium to its thermal value provides an independent method to measure the rates of equilibration.

### Introduction

Oxidation of aromatic amines by OH radicals to yield anilino-type radicals often proceeds through OH adducts either to the ring or to the amino group. The OH adducts then eliminate water or OH<sup>-</sup> to produce the anilino-type radicals or their acidic radical cations.<sup>1-3</sup> It was also noted that small yields of ammonia elimination can occur from the OH adduct of primary aromatic amines.<sup>1,4</sup> The variety of processes that may occur following the

addition of OH radicals to aromatic amines, including the elimination processes and establishing of acid-base equilibria, results in a rather complex kinetic behavior of these systems. This complexity may then lead toward erroneous identification of the intermediates involved and their optical spectra as has already been noted by Holcman and Sehested.<sup>3</sup> For the radicals discussed in the present report, diphenylamine radicals, the spectra previously reported and their assignment thus require verification. We therefore devoted some effort to clarifying the details of the reaction of OH radicals with diphenylamine (DPAH).

The focus of interest in the present study however is the photochemistry and photophysics of diphenylamine radicals. In previous reports we described in detail the photochemistry and

(1) Christensen, H. *Int. J. Radiat. Phys. Chem.* **1972**, *4*, 311.

(2) Rao, P. S.; Hayon, E. *J. Phys. Chem.* **1975**, *79*, 1063.

(3) Holcman, J.; Sehested, K. *J. Phys. Chem.* **1977**, *81*, 1963.

(4) Neta, P.; Fessenden, R. W. *J. Phys. Chem.* **1974**, *78*, 523.

photophysics of arylmethyl radicals at ambient temperatures in solution.<sup>5</sup> An extension of this study to the isoelectronic anilino-type radicals is quite interesting in an effort to systematically investigate the effect of the heteroatom on the behavior of the excited states of such short-lived intermediates. While diphenylmethyl radicals were found to possess a relatively long-lived ( $\tau = 280$  ns), highly fluorescent ( $\phi_f = 0.3$ ) lowest excited doublet state, this is not expected to be the case for diphenylamino radicals. The lifetimes of several excited anilino radicals have been recently measured to be  $\sim 12$  ns<sup>6</sup> (compare to  $1.4$   $\mu$ s for benzyl radicals<sup>7</sup>) at 77 K in glassy matrices. Considering the pronounced red shift and the increase in absorptivity when comparing diphenylamino radicals with anilino radicals, we can safely assume the lifetime for the former to be  $< 10$  ns. Similar circumstances have been experimentally verified when diphenylmethyl radicals are compared with benzyl radicals.<sup>5,7</sup> This short lifetime of the diphenylamino radical would exclude direct observation of the excited state with our present experimental facilities. However, its longer lived chemical consequences may persist long enough to be observable. In particular, one may expect different  $pK_a$  values for the amino radical in its excited state and its ground state. We therefore investigated the effects of excitation on diphenylamino radicals in aqueous solutions at various pHs. While we observe no photophysical or photochemical effects from the excitation of the amino radical, we found that excitation of its precursor, DPAH $\cdot$ -OH, does produce photochemical changes.

### Experimental Section

Diphenylamine was purified by repeated recrystallization. All other materials were of highest purity commercially available and were used without further purification. Water used was triply distilled, and all solutions were  $N_2O$  saturated by using the syringe technique.

Spectral analysis of the radicals produced by pulse radiolysis is done using the streak camera technique for detection.<sup>8a</sup> For more detailed kinetic analysis, a monochromator/photomultiplier combination was used. The conductivity detection technique, used to verify formation or decay of cations, has been previously described.<sup>8b</sup> The pulse radiolysis/laser flash photolysis system employed for the present study and the methods for actinometry and dosimetry have also been recently described.<sup>5b</sup> Briefly, radicals were produced by pulse radiolysis of aqueous solutions (4–40 ns linac pulses, 1–10 krad/pulse) and were then excited after a desired delay time by a frequency-doubled ruby laser pulse ( $\lambda_{exc} = 347$  nm,  $\leq 50$  mJ/pulse, 10-ns pulse width). The only addition to the previously described system<sup>5b</sup> is the application of a streak camera for the detection of the transients. While this addition overcomes problems associated with shot-to-shot variations in laser power or jitter in the linac-to-laser delay times, the sensitivity of the streak camera system is inferior to that of the photomultiplier detection.

The relatively low solubility of diphenylamine in water restricts the range of concentration accessible. For most of the experiments described below, saturated solutions were used. Excess diphenylamine was suspended in water and the solution allowed to stir at 40 °C for several hours. The saturated solution was then cooled to room temperature and then taken for the irradiation experiments after addition of the other solution components. We estimate the concentration of diphenylamine in the saturated solutions to be  $3 \times 10^{-4}$  M from spectrophotometric measurements. Solutions in the pH range  $4 < \text{pH} < 10$  contained either phosphate or borate buffers (except for conductivity measurements), the concentration of which was deliberately kept at  $(1-2) \times 10^{-4}$  M,

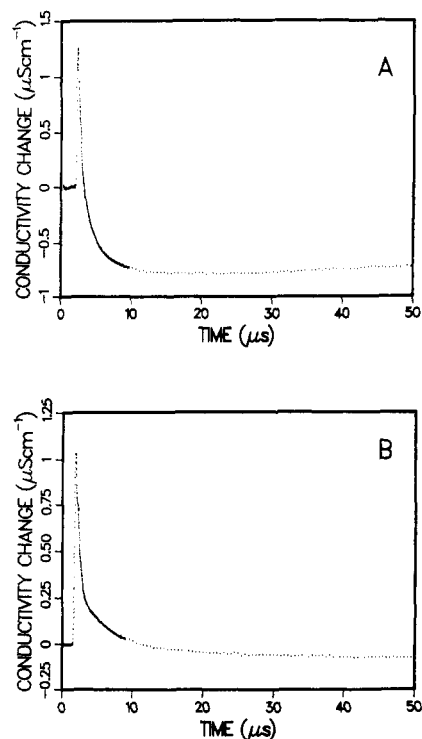


**Figure 1.** Conductivity signals following pulse radiolysis of DPAH-saturated solutions at pH 4.2 (A) and pH 9.5 (B); both solutions are also saturated with  $N_2O$ . Curves are normalized to 980 rad.

to avoid interference of direct reactions of the buffer.

### Results and Discussion

The primary radicals produced upon radiolysis of aqueous  $N_2O$ -saturated solutions are the OH radicals ( $G = 5.5$  radicals/100 eV). The contribution from the small amount of H atoms ( $G = 0.6$  radicals/100 eV) is neglected here.

**Conductivity Studies.** In an effort to determine the kinetics of the protonation/deprotonation reactions of the radicals produced upon the reaction of OH with DPAH, we resorted to the conductivity detection technique. Due to the high equivalent conductance of  $H^+$  and  $OH^-$  (350 and 198  $S\ cm^2\ equiv^{-1}$ , respectively), the signals observed following pulse radiolysis of aqueous solutions are primarily due to changes in concentrations of these two ions. Figure 1 displays the results obtained following irradiation of  $N_2O$ -saturated solutions of DPAH at pH 4.2 and 9.5. The initial increase and the following fast relaxation of the conductivity signals at both pHs are due to direct formation of  $H^+$ ,  $OH^-$ , and  $e_{aq}^-$  and their subsequent neutralization. At pH 4.2 the conductivity then continues to decrease at a slower rate to a level lower than the initial level (Figure 1A). This decay must be due to a protonation reaction of a DPAH radical species. The asymptotic amplitude of the negative part of the signal was calibrated to provide a measure for the yield of protonated radicals. These experimentally determined yields are shown in Figure 2A as a function of pH. The solid line in Figure 2A is a titration curve calculated by using  $G_{e_{aq}^-} = 2.8$  molecules/100 eV,  $G_{OH} = 2.7$  molecules/100 eV, and an equivalent conductance of the cation of 35  $S\ cm^2\ equiv^{-1}$ . The curve was corrected for the amount of  $e_{aq}^-$  reacting with  $H^+$  (rather than with  $N_2O$ ). The best-fitting titration curve yields a  $pK_a$  of  $4.25 \pm 0.1$  for this radical, close to the previously determined value.<sup>2</sup> The rate of the protonation reaction was measured as a function of  $[H^+]$  in the acidic pH range. As can be seen in Figure 2B, the protonation reaction proceeds through a pH-independent route with  $k_0 = 5.5 \times 10^5\ s^{-1}$  and in a parallel pH-dependent process of  $k_{H^+} = 0.9 \times 10^9\ M^{-1}\ s^{-1}$ . It may also be noted that, contrary to previous suggestions,<sup>2</sup> no dication is formed in the pH range 3–11 at times up to 200  $\mu$ s following the linac pulse. This conclusion results from the quantitative agreement between the calculated titration curve and the experimental points of Figure 2A. The formation

(5) (a) Bromberg, A.; Schmidt, K. H.; Meisel, D. *J. Am. Chem. Soc.* **1984**, *106*, 3056. (b) *J. Am. Chem. Soc.* **1985**, *107*, 83. (c) Bromberg, A.; Meisel, D. *J. Phys. Chem.* **1985**, *89*, 2507.

(6) Smirnov, V. A.; Brichkin, S. B.; Efimov, S. P. *High Energy Chem. (Engl. Transl.)* **1984**, *18*, 46.

(7) Okamura, T.; Obi, K.; Tanaka, I. *Chem. Phys. Lett.* **1973**, *20*, 90; **1974**, *26*, 218.

(8) (a) Schmidt, K. H.; Gordon, S. *Rev. Sci. Instrum.* **1979**, *50*, 1656. (b) Schmidt, K. H. *Int. J. Radiat. Phys. Chem.* **1972**, *4*, 439. Schmidt, K. H.; Gordon, S.; Thompson, M.; Sullivan, J. C.; Mulac, W. A. *Radiat. Phys. Chem.* **1983**, *21*, 321.

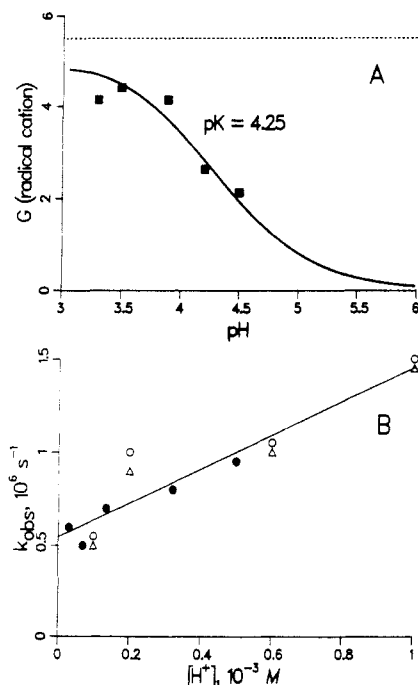


**Figure 2.** (A) Yield of the protonated radicals as a function of pH determined by the conductivity technique. Solid curve is best fit to the experimental points using the indicated  $pK_a$  and correcting for competition of  $H^+$  for  $e_{aq}^-$ ; dashed line is the theoretical yield when  $e_{aq}^-$  is completely scavenged by  $N_2O$ . (B) Rate of the protonation reaction as a function of  $[H^+]$ : (●), conductivity results; (○), formation at  $\lambda = 670$  nm; (Δ), decay at  $\lambda = 360$  nm.

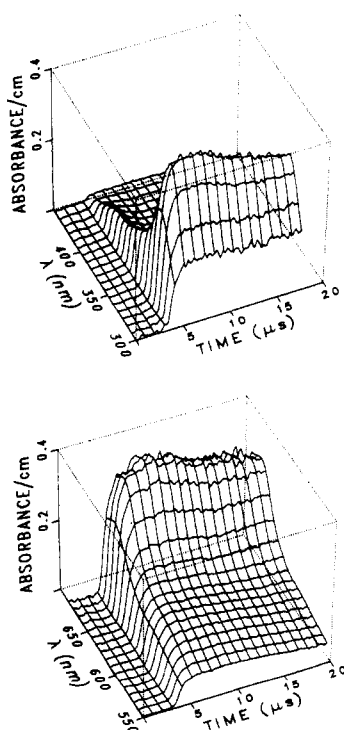


**Figure 3.** Three-dimensional representation of the results obtained on pulse radiolysis of DPAH solution at pH 3 using the streak camera detection technique.

of a dication would result in larger negative signal amplitudes.

Results from the conductivity experiments at the basic pH range provide further insight into the acid-base equilibria of this system. As can be seen in Figure 1B after the initial neutralization is complete, an increase of conductivity above the prepulse level persists and decays relatively slowly with an observed rate constant of  $k_{obsd} \approx 3.0 \times 10^5 \text{ s}^{-1}$ . This decay, however, does not fit a pure first-order rate law. Extrapolation of this slowly decaying signal

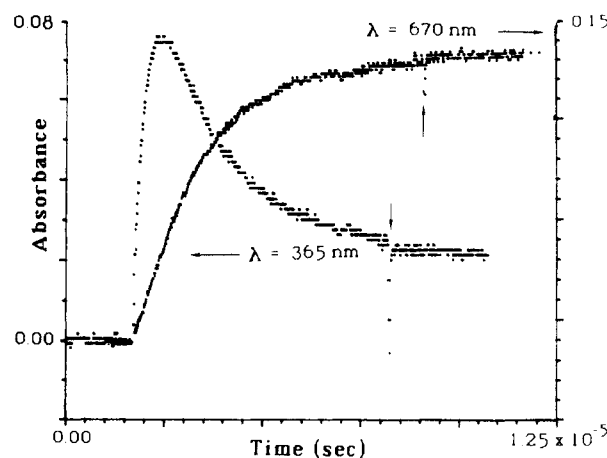
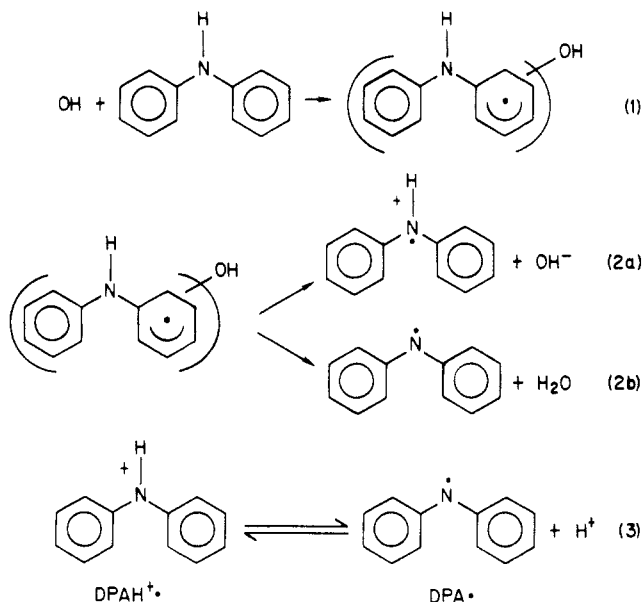


**Figure 4.** Kinetic traces for formation and decay of species absorbing at  $\lambda = 365$  and  $670$  nm;  $N_2O$ -saturated DPAH solution at pH 3.5. Vertical arrows show timing of laser pulse to indicate hardly any laser effects at these times.

to the center of the pulse yields  $G \approx 1.4$  molecules/100 eV. As will become clear from the spectrophotometric results described below, this yield and the slow decay are a composite of two processes. The rate of decay is therefore distorted, and the yield of 1.4 molecules/100 eV, is, therefore, only a lower limit. The significance of this observation is, however, in the conclusion that a substantial yield of  $OH^-$  is released directly to the solution in this basic pH range.

In discussing the processes observed following DPAH irradiation, we refer to the following sequence of reactions:



The product of reaction 1 is depicted to denote the OH addition products where the site of addition might be any combination of the four possible sites. From the conductivity results in the basic range, we conclude that reaction 2a occurs to a substantial degree. The  $pK_a$  determination in Figure 2A probably refers to equilibrium 3. The protonation process observed in Figures 1A and 2B might, however, refer either to the establishment of equilibrium 3 or to an acid-catalyzed reaction 2. The spectrophotometric results described below verify the  $pK_a$  determination and point to the latter interpretation.

**Spectrophotometric Studies.** Figure 3 presents results from the streak camera technique obtained upon irradiation of DPAH solutions at pH 3. For detailed analysis, we chose only a few spectral regions for kinetic study using the photomultiplier detection technique at various pHs. Typical kinetic traces are shown in Figure 4 for the acidic pH range. Comparison of the two traces in Figure 4 clearly indicates that the rate of formation of the

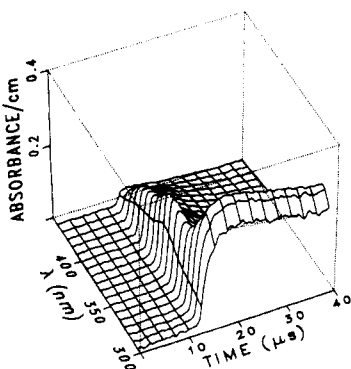


Figure 5. Streak camera results from irradiation of DPAH at pH 9.

species absorbing the 670 nm is slower than the formation of the species absorbing in the UV region and actually parallels the decay of the latter species. When the DPAH concentration is lowered by a factor of 10 (at pH 3.0), the rates of formation of the red absorption and the UV absorption are equal. Furthermore, the absorption in the UV range grows to the same final level observed in Figure 4 without going through the decaying intermediate seen in Figure 4. This observation indicates that the decaying intermediate observed in Figure 4 is a precursor which decays to produce the second intermediate. At the low concentration, the rate-determining step is the rate of formation of the primary radical and the rate of its transformation to the second radical is faster than the former rate.

The fast rate of formation of the radical absorbing in the UV region was found to be pH independent (pH 3–9) and is therefore attributed to the formation of the OH adduct. The rate constant for this reaction was measured to be  $k_1 = 1.0 \times 10^{10} \text{ M}^{-1} \text{ s}^{-1}$ . No absorbance attributable to the product of this reaction in the red region of the spectrum could be observed. The rate of formation of the absorption in the red region and the rate of the decay in the UV region were found to depend on pH in the acidic range. A plot of this dependence on pH yields similar results to those obtained from the conductivity technique, with the same values within experimental error for the intercept and slope (Figure 2B). The absorbance at 670 nm at the end of the formation reaction was measured as a function of pH, and its pH dependence was found to follow the same  $\text{pK}_a$  curve as the conductivity results (Figure 2A). We therefore conclude that Figures 1A and 4 illustrate the same process which necessarily is a formation of a cation. That this cation is the amino radical cation,  $\text{DPAH}^+$ , was verified by comparing the absorption spectrum at the end of this reaction with the spectrum obtained from the reaction of DPAH with  $\text{Br}_2^-$  radicals. The latter reacts with DPAH to form directly the amino radical cation ( $k(\text{Br}_2^- + \text{DPAH}) = 2.2 \times 10^9 \text{ M}^{-1} \text{ s}^{-1}$ ). Since  $\text{Br}_2^-$  is known to react exclusively by electron-transfer routes with a wide variety of substrates, we conclude from the similarity of the spectra that the same radical cation is produced in both systems.

Streak camera results from irradiation of  $\text{N}_2\text{O}$ -saturated DPAH solutions in the basic pH range are shown in Figure 5. Detailed kinetic traces at the same wavelengths studied in the acidic range are shown in Figure 6 for pH 9.2. The same rate constants and the same yields were obtained in the pH range 9–10. While the absorbance at 670 nm is substantially lower in the basic pH range than in the acidic range, the rate of its buildup is faster in the basic range. As can be seen in Figure 6, the rate of formation of absorbance in the red spectral range is similar to the rate of formation in the UV range. It can also be noted in Figure 6 that, while the decay of absorption at 365 nm has the same rate constant as given by the intercept of Figure 2B, no further buildup (or decay) of the absorption at 670 nm is observed. Two explanations may be considered to rationalize both these observations. It may be argued that the fast formation of absorption in the red region of the spectrum is due to absorption by  $\text{DPAH}\cdot\text{OH}$  in this region. This would require, then, that 670 nm is an isosbestic point for  $\text{DPAH}\cdot\text{OH}$  and  $\text{DPA}\cdot$ . Since hydroxycyclohexadienyl radicals

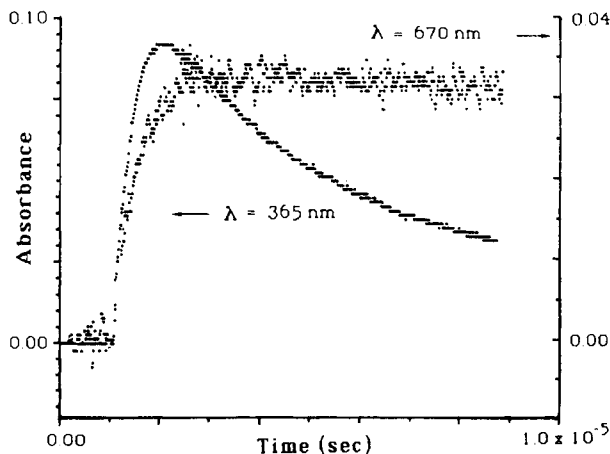
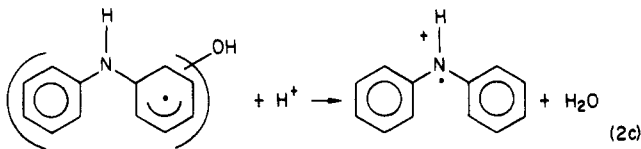


Figure 6. Kinetic traces for formation and decay of the species absorbing at 365 and 670 nm.  $\text{N}_2\text{O}$ -saturated DPAH solution at pH 9.2.

in general do not absorb light in the red, this explanation seems unlikely. The other explanation requires fast  $\text{OH}^-$  elimination from one of the OH adducts (e.g., of the adduct at the position  $\alpha$  to the nitrogen and perhaps base catalyzed). This will produce originally the radical cation which absorbs strongly in the red spectral region. Concomitant with the following deprotonation of  $\text{DPAH}^+$  (reaction 3), further  $\text{OH}^-$  elimination from the other positions may occur, resulting in little change in absorbance at 670 nm. In support of this suggestion, we note that the rate of  $\text{OH}^-$  elimination,  $k_{2a}$ , from the majority of the OH adducts is similar to the deprotonation rate,  $k_3$ . The latter rate constant is determined in the following section. That the amino radical does absorb in the red with low absorptivity has been verified by direct oxidation of DPAH by  $\text{Br}_2^-$  radicals at pH 9.

In summary, the above analysis leads to the conclusion that the reaction characterized by the rate constants of Figure 2B is actually a combination of reaction 2a and an acid-catalyzed dehydration reaction 2c, i.e.,  $k_{2a} = 5.5 \times 10^5 \text{ s}^{-1}$  and  $k_{2c} = 0.9$



$\times 10^9 \text{ M}^{-1} \text{ s}^{-1}$ . From the value of  $k_{2a}$  thus obtained and from the previously proposed correlation between the ionization potential of several substituted benzenes and the rate constant of  $\text{OH}^-$  elimination from the OH adduct,<sup>9</sup> one obtains  $I_p = 7.5 \text{ eV}$  for the ionization potential of DPAH. Values in the literature are in the range of  $I_p = 7.25\text{--}8.0 \text{ eV}$ .<sup>10</sup> The acid-catalyzed route for  $\text{OH}^-$  elimination has been demonstrated for a large number of OH adducts to aromatic compounds.<sup>11</sup> It may be also noted that the value of  $k_{2c}$  determined above is somewhat too low to be interpreted as a protonation reaction of an acid–base equilibrium.

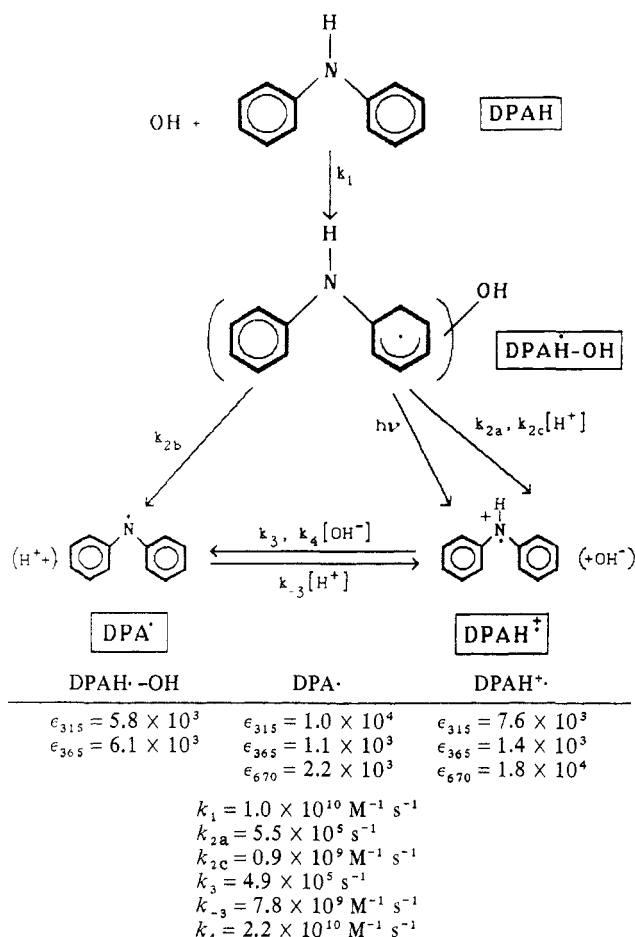
While the OH adduct to DPAH may be formally considered to be the conjugated base of the radical cations,  $\text{DPAH}^+$ , no attempt was made to observe the reverse of reaction 2a. In addition to severe technical limitations to the design of such an experiment, the reaction of  $\text{OH}^-$  with the radical cation is expected to lead to deprotonation and formation of the neutral  $\text{DPA}\cdot$  radical. This point, as well as the whole scheme of reactions outlined above, is reinforced by the excitation experiments described below. In Scheme I we summarize our observations made so far on this system along with the observations from the excitation experi-

(9) Holcman, J.; Sehested, K. *Nukleonika* **1979**, *24*, 887.

(10) (a) Becker, F. *Chem. Ber.* **1953**, *86*, 1150. (b) Vilesov, F. I.; Zaitsev, V. M. *Dokl. Phys. Chem. (Engl. Transl.)* **1964**, *154*, 117.

(11) (a) Sehested, K.; Hart, E. J. *J. Phys. Chem.* **1975**, *79*, 2773. (b) Zevos, N.; Sehested, K. *J. Phys. Chem.* **1978**, *82*, 138. (c) O'Neill, P.; Steenken, S.; Schulte-Frohlinde, D. *J. Phys. Chem.* **1977**, *81*, 31. (d) Sehested, K.; Holcman, J.; Hart, E. J. *J. Phys. Chem.* **1977**, *81*, 1363. (e) Steenken, S.; O'Neill, P.; Schulte-Frohlinde, D. *J. Phys. Chem.* **1977**, *81*, 26.

## SCHEME I



ments. While we were unable to determine a rate constant for reaction 2b, some contribution from this pathway cannot be complete excluded. Any contribution from this reaction to the rate of DPAH-OH decay is included in the intercept of Figure 2B. The pulse radiolysis experiments alone do not allow determination of the rate of the acid-base equilibration of reaction 3. The excitation experiments described in the following section provide detailed information on this reaction.

**Excitation of the Radicals.** By use of the pulse radiolysis/flash photolysis combination described in the Experimental Section, each of the radicals originating in DPAH has been excited with the frequency-doubled ruby laser pulse. As already mentioned in the Introduction, the lifetime of the doublet excited state of the amino radical is expected to be shorter than our experimental time resolution. Indeed, no fluorescence or absorption that could be attributed to an excited state of either the neutral amino radical or its acid cationic form could be observed following excitation of the corresponding ground-state radicals. This has been verified for both DPA· and DPAH· radicals produced either by  $\text{Br}_2^-$  oxidation or by the OH reaction in the pH range 3–11. We further failed to observe any persistent changes (longer than  $\sim 20$  ns) in the absorption spectra of the amino radicals and radical cations which would result from different  $pK_a$ 's of the excited state as compared to the ground state (e.g., see Figure 4). This point requires some elaboration. The  $pK_a^*$  values of a large number of excited singlet states of aromatic amine derivatives have been shown to be some 5–8 pH units smaller than that of the ground state.<sup>12</sup> If the same trend is preserved in the first excited doublet state of the radicals (i.e.,  $pK_a^*(D_1) \ll pK_a(D_0)$ ), then excitation

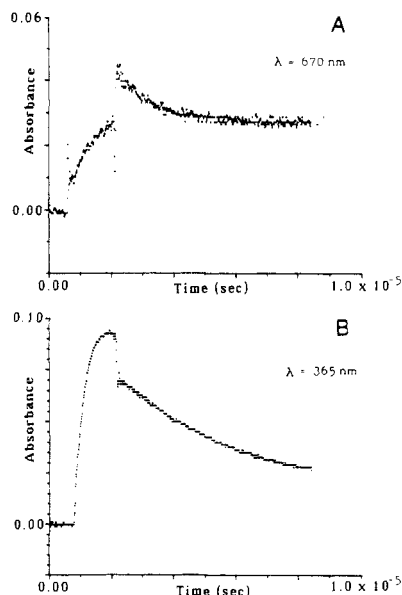


Figure 7. Excitation of the OH adduct at pH 9.2: (A) detection at 670 nm; (B) detection at 365 nm.

of the radical cation at pHs close to its  $pK_a$  should lead to deprotonation of the excited state. The relaxation of the ground-state acid-base equilibrium might then be observed with our experimental arrangement. We, however, observed no such reequilibration. This lack of excitation effect may result from a  $pK_a^*$  which is not very different from the ground-state  $pK_a$ . Using a Förster cycle and taking the maxima in the absorption spectra of the radical and its conjugated acid (700 and 670 nm, respectively), we obtain  $pK_a^*(D_1) = 2.8$ . This implies a relatively small difference in  $pK_a$  between the ground and the first excited doublet state. Such small changes are typical of the change in  $pK_a$  on excitation to the lowest triplet state, rather than the first excited singlet state, in the parent amine molecules (e.g.,  $pK_a(S_0) = 4.41$ , while  $pK_a(T_1) = 3.3$  for 2-naphthylamine;<sup>13a</sup> note that similar comparisons for DPAH are impractical due to its low  $pK_a(S_0) = 0.79$ ). The relatively high  $pK_a^*(D_1)$  then will lead to a deprotonation rate which is much slower than the expected lifetime of the excited radical. If we assume an upper limit for the rate constant of protonation of the excited state which is equal to that of the ground state ( $k_{-3} = 7.8 \times 10^9 \text{ M}^{-1} \text{ s}^{-1}$ , determined below), the above  $pK_a^* = 2.8$  yields  $1.2 \times 10^7 \text{ s}^{-1}$  for the deprotonation rate constant of the excited state in the absence of a base. This is at least an order of magnitude slower than the expected decay rate of the excited state. The often invoked theory of mixing higher charge-transfer configurations in the lowest excited state may be applied here.<sup>14</sup> The relatively small  $\Delta pK_a(D_0-D_1)$  then implies only a small contribution from such charge-transfer states. As in the case of triplets, this probably results from a large energy gap between  $D_1$  and the charge-transfer states. We note in passing that a Förster cycle based on the absorption maxima of the anilino radical and its conjugated radical cation (400 and 425 nm, respectively)<sup>13b</sup> would actually predict an increase from  $pK_a(D_0) = 7.0$  to  $pK_a^*(D_1) = 10$ , indicating an increased electron density at the nitrogen atom in the excited state.

While no laser excitation effect could be observed on the amino radicals, pronounced effects on the transient absorptions could be observed when the excitation occurs before formation of the amino radicals is complete. Such effects are shown in Figure 7. Using a series of neutral density filters to attenuate the laser light intensity, we have verified that these excitation effects are monophotonic. The magnitude of the absorption change following the laser pulse decreases when the linac-to-laser delay is increased

(12) (a) Weller, A. In "Progress in Reaction Kinetics"; Porter, G., Ed.; Pergamon Press: New York, 1961; Vol. 1, p 189. (b) Vander Donckt, E. In "Progress in Reaction Kinetics"; Pergamon Press: New York, 1970; Vol. 5, p 273. (c) Sengupta, D.; Lahiri, S. C. *Z. Phys. Chem. (Leipzig)* **1977**, *258*, 1097.

(13) (a) Jackson, G.; Porter, G. *Proc. R. Soc. London, A* **1961**, *200*, 13. (b) Land, E. J.; Porter, G. *Trans. Faraday Soc.* **1963**, 2027.

(14) Murrell, J. N. "The Theory of Electronic Spectra of Organic Molecules"; Methuen: London, 1963.

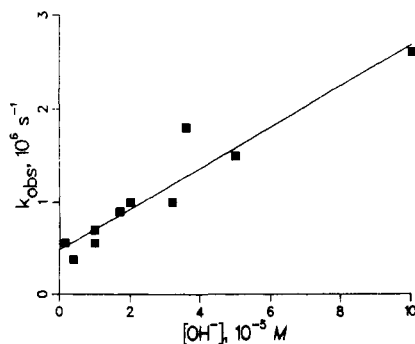
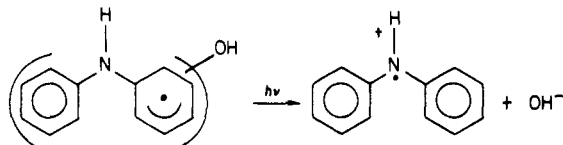


Figure 8. The observed rate constant for the decay of the absorption formed at 670 nm by the laser excitation, as a function of  $[\text{OH}^-]$ .

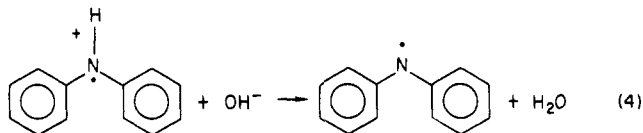
or decreased relative to the one shown in Figure 7. This timing dependence leads us to believe that the radical excited is the OH adduct, in accordance with the interpretation given above. At very short linac-to-laser delays very little of the adduct has been formed, while at long delays, a large fraction of the adduct has already been converted to the amino radicals. The rate of the decay of the absorption formed by the laser pulse at 670 nm increases with  $[\text{OH}^-]$  in the pH range 9–10 (Figure 8). In the acid pH range 3–4 as well as at pH 11, the laser-induced absorption change at any wavelength is always in the same direction as the direction of the thermal reaction without any further change. The difference in spectra immediately before and after the laser pulse resembles the difference spectrum between the OH adduct and the neutral amino radical at pH 11; it, however, resembles the difference spectrum between the OH adduct and the amino radical cation at pH 3–10. It may also be noted that no recovery following the laser excitation is observed in the UV range (Figure 7B) due to the resemblance of the spectra of the three radicals involved in this range and the thermal kinetics imposed on the system.

All these observations, we believe, can be explained by assuming that excitation of the OH adduct leads to  $\text{OH}^-$  elimination from the excited state of that radical:



The observed behavior of the absorption signals will then depend on the kinetics of the dark reactions that follow. The effect of the laser thus amounts to a laser-induced perturbation of an acid–base equilibrium.<sup>15</sup> Using the same actinometer system previously described,<sup>5b</sup> we estimate a quantum yield of  $0.15 \pm 0.05$  for this process. Regardless of the lifetime of the excited state of the OH adduct radical, it is assumed here that the  $\text{OH}^-$  elim-

ination is instantaneous on the time scale of the experiment, and thus only ground states of the radicals are observed, albeit not necessarily at thermal acid–base equilibrium. The rate constants shown in Figure 8 will then refer to  $k_4 = 2.2 \times 10^{10} \text{ M}^{-1} \text{ s}^{-1}$  (slope in Figure 8) and  $k_3 = 4.9 \times 10^5 \text{ s}^{-1}$  (intercept). From the  $\text{p}K_a = 4.2$  of the amino radical, we also estimate  $k_{-3} = 7.8 \times 10^9 \text{ M}^{-1} \text{ s}^{-1}$ . The rate constant derived here for reaction 4 is well within



the range of rates for hydroxyl ion reactions with protonated amines.<sup>16</sup> The somewhat slower than usual rate constant for protonation,  $k_{-3}$ , probably reflects the strong delocalization of the unpaired electron into the phenyl rings.

### Conclusion

Two goals were the main focus of the present report. In view of the conflicting reports regarding the reaction of OH radicals with aromatic amines,<sup>2,3</sup> we tried to clarify the identity of the intermediates of this reaction with DPAH. We differ in the details of the various routes leading from the OH adduct (obviously a mixture of adducts) to the amino radicals reported previously<sup>2</sup> and assignment of the absorption spectrum to the adduct. We conclude, however, that the assignment of the optical spectra to the two amino radicals,  $\text{DPA}^\bullet$  and  $\text{DPAH}^{+\bullet}$ , is essentially corrected. The other interest stems from our effort to obtain some information on the photophysics and photochemistry of radicals in solution. Whereas the lifetimes of the excited anilino-type radicals of DPAH are too short to measure with our experimental apparatus, the lack of any laser-induced  $\text{p}K_a$  perturbation effect leads us to conclude that the difference in the  $\text{p}K_a$  of the lowest excited doublet state and the ground state of these radicals is rather small. This was further substantiated by Förster cycle considerations using the absorption maxima of the neutral radical and the radical cation in the red region of their spectra. Photochemistry was, however, observed following excitation of the OH adduct. Since this photochemistry leads to photoelimination of  $\text{OH}^-$  and thus creates a thermally nonequilibrated population of the acid–base species, it provides an independent means for measuring the relaxation of these species to the thermal equilibrium.

**Acknowledgment.** The dedicated operation of the linac by D. Ficht and G. Cox is much appreciated. We thank P. Walsh and R. Clarke for technical assistance. This work was performed under the auspices of the Office of Basic Energy Sciences, Division of Chemical Science, U.S. DOE, under Contract No. W-31-109-ENG-38.

**Registry No.**  $\text{Ph}_2\text{NH}$ , 122-39-4;  $\text{HO}^\bullet$ , 3352-57-6.

(15) Huppert, D.; Gutman, M.; Kaufmann, K. J. *Adv. Chem. Phys.* **1981**, *47*, 643.

(16) Eigen, M. In "Fast Reactions and Primary Processes in Chemical Kinetics"; Claesson, S., Ed.; Interscience: New York, 1967; p 245.